Journal Pre-proof

The Renin-Angiotensin-Aldosterone System (RAAS) is One of the Effectors by Which Vascular Endothelial Growth Factor (VEGF)/anti-VEGF Controls the Endothelial Cell Barrier

Yueru Li, Zhonghao Yan, Komal Chaudhry, Andrius Kazlauskas

PII: S0002-9440(20)30295-9

DOI: https://doi.org/10.1016/j.ajpath.2020.06.004

Reference: AJPA 3392

To appear in: *The American Journal of Pathology*

Received Date: 3 March 2020

Revised Date: 23 May 2020

Accepted Date: 1 June 2020

Please cite this article as: Li Y, Yan Z, Chaudhry K, Kazlauskas A, The Renin-Angiotensin-Aldosterone System (RAAS) is One of the Effectors by Which Vascular Endothelial Growth Factor (VEGF)/anti-VEGF Controls the Endothelial Cell Barrier, *The American Journal of Pathology* (2020), doi: https://doi.org/10.1016/j.ajpath.2020.06.004.

This is a PDF file of an article that has undergone enhancements after acceptance, such as the addition of a cover page and metadata, and formatting for readability, but it is not yet the definitive version of record. This version will undergo additional copyediting, typesetting and review before it is published in its final form, but we are providing this version to give early visibility of the article. Please note that, during the production process, errors may be discovered which could affect the content, and all legal disclaimers that apply to the journal pertain.

Copyright © 2020 Published by Elsevier Inc. on behalf of the American Society for Investigative Pathology.

Journal Pre-proof

The Renin-Angiotensin-Aldosterone System (RAAS) is One of the Effectors by Which Vascular Endothelial Growth Factor (VEGF)/anti-VEGF Controls the Endothelial Cell Barrier

Yueru Li[1], Zhonghao Yan[1], Komal Chaudhry[3] and Andrius Kazlauskas[1,2*]

University of Illinois at Chicago

Department of Ophthalmology & Visual Sciences[1]

Department of Physiology and Biophysics[2]

1905 West Taylor St

Chicago, IL 60612

Southern Illinois University School of Medicine[3]

Carbondale, IL 62901

*** corresponding author**
Andrius Kazlauskas
University of Illinois at Chicago
Lions Illinois Eye Research Institute
1905 W Taylor St.; Room 245
Chicago, IL 60612
781-475-9479 (phone)
312 996-7770 (fax)
ak20@uic.edu

Number of text pages: 27. Number of tables: 1. Number of figures: 5. Number of supplementary figures: 5. Number of supplementary tables: 1

Running Title:

RAAS, VEGF/anti-VEGF, permeability

Sources of support:

UIC start-up funds, A.K. JDRF 2-SRA-2019-856-S-B, A.K. ISPB, Y.L. NIH UL1TR002003 (UIC bioinformatics).

Disclosures: None declared.

Journal Pre-proof

Journal Pre-proof

Abstract

Leakage of retinal blood vessels, which is an essential element of diabetic retinopathy (DR), is driven by chronic elevation of vascular endothelial growth factor (VEGF). VEGF quickly relaxes the endothelial cell barrier by triggering signaling events that post-translationally modify preexisting components of intercellular junctions. VEGF also changes expression of genes, which are known to regulate barrier function. This project's goal was to identify effectors by which VEGF and anti-VEGF control the endothelial cell barrier in cells that were chronically exposed to VEGF (hours instead of minutes).

We discovered that the duration of VEGF exposure influenced both barrier relaxation, and anti-VEGF-mediated closure. Most VEGF-induced changes in gene expression were not reversed by anti-VEGF. Those that were constitute VEGF effectors that are targets of anti-VEGF. Pursuit of such candidates revealed that VEGF used multiple, non-redundant effectors to relax the barrier in cells that were chronically exposed to VEGF. One such effectors was ACE (angiotensin converting enzyme), which is a member of the renin-angiotensin aldosterone system (RAAS). Pharmacologically antagonizing either ACE, or the receptor for angiotensin II, attenuated VEGF-mediated relaxation of the barrier. Finally, activating the RAAS reduced the efficacy of anti-VEGF. These discoveries provide a plausible mechanistic explanation for the long-standing appreciation that RAAS inhibitors are beneficial for patients with DR and suggest that antagonizing the RAAS improves patients' responsiveness to anti-VEGF.

Journal Pre-proof

Introduction

In 2013 approximately 1 out of 19 people had diabetes mellitus (DM). The incidence of this life-long affliction is increasing: 1 of every 14 people are predicted to have DM in 2030 [1]. This metabolic disease causes both macrovascular and microvascular dysfunction, which manifests in multiple organs (eyes, kidneys, skin, et al.) and systems (e.g. cardiovascular, neural, et al.) [2]. Thus, a substantial percentage of our world's population has diabetes, and their quality of life is compromised by the complications that they develop.

Approximately 1/3 of patients with diabetes have diabetic retinopathy (DR) [3, 4], which is diagnosed and staged based on the anatomy of the retinal vasculature, the thickness of both individual layers within the retina, and the total retina. High blood pressure is one of the risk factors for developing DR [5], and medications that control blood pressure reduce the risk of developing DR, and increase the likelihood of regression [6, 7]. These benefits have been reported for patients taking antagonists of the renin angiotensin aldosterone system (RAAS), which include inhibitors of ACE (angiotensin converting enzyme) (such as ramipril and trandolapril), and angiotensin II (AII) receptor antagonists (such as valsartan and telmisartan). The key elements of the RAAS include renin-mediated cleavage of angiotensin I, which ACE proteolyzes to generate the 8 amino acid AII that binds to G protein-coupled receptors such as AGTR1 (angiotensin II receptor 1) [8, 9]. Thus, RAAS antagonists, which reduce the activity of ACE or AII-dependent activation of AGTR1, are beneficial for patients with DR.

Animal models of DR can reproduce this clinical phenomenon. Antagonizing the RAAS prevents diabetic rodents from developing DR [10-13]. Systemic administration of RAAS inhibitors have no effect on DM, yet they prevent leakage of retinal blood vessels, a hallmark of DR. Animals treated in this way also have lower levels of retinal VEGF (vascular endothelial growth

factor A), which could result from not developing DR. Alternatively, antagonizing the RAAS may prevent the DM-driven rise in VEGF, which promotes DR. The underlying mechanism by which RAAS inhibitors protect experimental animals from DR and are beneficial in patients has not been addressed.

Neutralizing retinal VEGF is one of the ways that patients with DR are treated. While many patients with DR benefit from anti-VEGF, the response is not uniform [14-17]. A recent report, which indicates that genetic variants in the RAAS predict response to anti-VEGF in cancer patients [18], raises the intriguing question of whether consumption of RAAS antagonists affects the efficacy of anti-VEGF administered to patients with DR.

In this study we investigated how VEGF/anti-VEGF controlled permeability of primary human retinal endothelial cells that were enduringly exposed to VEGF. We discovered that VEGF increased, and anti-VEGF decreased expression of *ACE*, a driver of the RAAS. Antagonists of the RAAS partially suppressed VEGF-mediated relaxation of the barrier indicating that VEGF uses multiple effectors to relax the barrier, and that the RAAS is one of them. Finally, enforced activation of RAAS attenuated anti-VEGF's ability to reclose the barrier. These results provide mechanistic insights regarding the relationship between RAAS and VEGF/anti-VEGF-dependent control of endothelial cell barrier, which are relevant to current management of patients with DR.

Materials and Methods

Materials

Human retinal endothelial cells (HRECs) were purchased from Cell Systems (ACBRI 181) (Kirkland, WA). They were derived from donor A, a 26-year old Caucasian male. Lonza

endothelial cell basal medium-2 (EBM-2, CC3156) and Lonza SingleQuots endothelial cell growth medium-2MV (EGM-2MV, CC4147) for tissue culture was procured from Lonza Bioscience (Verviers, Belgium). D-(+)-Glucose (G7021), recombinant human angiotensin converting enzyme (ACE, SAE0075), recombinant human angiotensin II (AII, A9525), ramipril (ACE inhibitor, R0404), trandolapril (ACE inhibitor, T4827), valsartan (AGTR1 inhibitor, SML0142), telmisartan (AGTR1 inhibitor, T8949), FITC-Dextran (70 KDa) and Celite 545 (22140) were purchased from Sigma. Recombinant human IL-1β (200-01B) was purchased from PeproTech, Inc. (NJ, USA). Recombinant human VEGF-A (VEGF 165; 293-VE) and human TNF-alpha Protein (210-TA) were purchased from R&D systems (MN, USA). Aflibercept (EYLEA) and bevacizumab (Avastin) were from Regeneron Pharmaceuticals, Inc. and Genentech, Inc, respectively. RNeasy Plus mini kit used for RNA isolation was obtained from QIAGEN (Hilden, Germany). High Capacity cDNA Reverse Transcription Kit used for cDNA synthesis and Fast SYBR Green Master Mix used for real-time PCR were purchased from Applied Biosystems (Thermo Fisher Scientific). Transwell 24-Well Permeable Support System used for FITC-Dextran permeability assay was purchased from Corning, Inc. (3391, ME, USA). Disposable Electrode Arrays (8W10E+ PC) used in transendothelial electrical resistance (TEER) assay for measuring cellular permeability were purchased from ECIS Cultureware (Applied BioPhysics, Inc, Troy, NY). Palmitic acid (N-16-A) was from NU-CHEK-PREP, INC., Elysian, MN.

Culture of human retinal endothelial cells

Primary human retinal microvascular endothelial cells (HRECs, Cell System, Kirkland, WA, USA) were used to establish an in vitro model of DR. HRECs were cultured in complete Lonza

medium (EBM-2 supplemented with the EGM-2MV SingleQuots kit). High glucose treated-cells HRECs were generated by culturing cells in complete Lonza medium containing 30 mM D-glucose for at least 10 days; medium was changed every 24 hrs. The second model of DM was generated by exposing high glucose-treated cells to palmitate (50 uM) and TNFα (0.1 ng/ml) for 24 hrs prior to the start of the experiment.

Palmitate was added to complete Lonza medium by first loading it with BSA as described by Spector and Hoak [19]. Briefly, palmitic acid dissolved in hexanes was coated onto Celite, the hexanes were evaporated under nitrogen, complete Lonza medium containing sufficient BSA to achieve a 5:1 molar ratio was then added (palmitic acid:BSA) and incubated for 30 min at room temperature. The Celite was removed by centrifugation, the pH of the supernatant was adjusted to 7.4, filtered through a 0.22 u filter and frozen until use.

Library preparation and RNA-seq

RNA-seq libraries of poly (A) RNA from 500 ng total RNA obtained from HRECs treated with vehicle, VEGF and VEGF + anti-VEGF were generated using the Clontech SMARTer Stranded RNA-Seq Kit (634838) for Illumina HiSEQ4000 (single end 50p). Fastq were generated using Illumina provide demultiplexing software.

RNAseq QC and quantification

RNAseq analysis was performed by the UIC or University of Chicago Core Facilities. Raw reads were aligned to reference genome hg38 using BWA MEM [20]. Genes was quantified using FeatureCounts [21] as raw read counts. Differential expression statistics (fold-change and p-value) were computed using edgeR [22, 23]. Multi-group statistics were computed using edgeR's

generalized linear modeling (GLM) framework, and pair-wise comparisons were computed using exactTest. In all cases we adjusted p-values for multiple testing using the false discovery rate (FDR) correction of Benjamini and Hochberg [24]. Differences in expression were considered statistically significant based on an FDR threshold of 5% (0.05). Bioinformatics analysis in the project described was performed by the UIC Research Informatics Core.

Clustering and visualization

We identified distinct and robustly separable genomic patterns using a discovery clustering analysis that pairs k-means clustering with reproducibility clustering statistics. We overcame inherent limitations in k-means clustering – that requires a priori selection of the number of clusters k and gives variable results with different initializations – by assessing cluster reproducibility. In particular, we performed k-means clustering with ten random initializations on a range of cluster numbers k (2 to 20). For each k, we evaluated the reproducibility of the repeated clustering runs using the Rand Index, similar to the approach outlined by Senbabaoglu and co-workers [25]. We then chose the largest k that yields highly reproducible clusters. Patterns from clusters were visualized using heatmaps and boxplots to aid in interpretation.

Pathway analysis

Gene sets obtained from the hierarchical clustering were analyzed in MetaCore using the Pathway Maps tool.

PCR analyses

HRECs were seeded at full confluency. VEGF was added to a final concentration of 2 nM and then cultured for an additional 0.5, 1.5 or 8 h. For the anti-VEGF group, after 8 h of VEGF incubation, aflibercept (1 uM) was added for an additional 8 h. The cells were the lysed, mRNA was isolated and used to synthesize cDNA. Quantitative PCR was performed using the real-time PCR HT7900 system (Applied Biosystems, Thermo Fisher Scientific, USA). The threshold cycle (Ct) of each transcript was normalized to the average Ct of the housekeeping genes (β-actin and GAPDH). Fold differences were determined by the 2-ΔΔCt method.

Western Blot

HRECs that were pre-incubated with vehicle or VEGF (1 nM) for 24 h were treated with anti-VEGF (Aflibercept) for indicated time periods. The cells were then rinsed with ice-cold PBS (phosphate buffered saline; 137 mM NaCl, 2.7 mM KCl, 8 mM Na_2HPO_4, and 2 mM KH_2PO_4) and lysed in electrophoresis sample buffer (10 mmol/L EDTA; 4% sodium dodecyl sulfate; 5.6 mol/L 2-mercaptoethanol; 20% glycerol; 200 mmol/L Tris-HCl, pH 6.8; and 0.2% bromophenol blue). Proteins were resolved on a 10% sodium dodecyl sulfate–polyacrylamide gel and subjected to Western blot analysis.

FITC-Dextran assay measuring cellular permeability

Cellular permeability in HRECs was measured according to the manufacturer's instruction. Specifically, HRECs were seeded at full confluency onto gelatin-coated 24-transwell inserts (0.4 μm polyester membrane, Corning). The cells were then pre-incubated with ACE inhibitors (ramipril, trandolapril) or AGTR1 inhibitor (valsartan) for 2 hours. After pre-treatment, HRECs were stimulated with VEGF (2 nM) overnight and monolayer solute permeability was

determined by addition of a 70-KDa molecular weight FITC-Dextran (Merck Millipore) and subsequent measurement of fluorescence intensity using a Synergy HTX microplate reader (BioTek). Fluorescence intensity was measured in duplicate per condition and normalized to untreated control cells.

Transendothelial electrical resistance (TEER) measuring cellular permeability

Cell permeability was assessed by measuring changes in TEER using ECIS (electrical cell-substrate impedance sensing, Applied Biophysics, Troy, NY). HRECs were seeded at full confluency in 8-well chamber slides equipped with gold-coated micro-electrodes. The electric current passing through the endothelial monolayers was measured independently in each chamber. TEER was measured continuously and in real time before, during and after the treatment of the cells. When RAAS inhibitors (ramipril, trandolapril, valsartan and telmisartan) were used, they were added 2 h before addition of VEGF.

Statistical Analysis

The results are expressed as mean ± SD. Differences among groups were evaluated by ANOVA; statistical significance of differences between groups was assessed using the student's t-test when indicated. Correlations between indicated variables were assessed using Pearson moment product correlation coefficients. Significance was defined as $P < 0.05$. Graphs were created using Microsoft Excel 2019, R (R Core Team 2019).

Results

VEGF/anti-VEGF control barrier function of HRECs

To investigate how VEGF/anti-VEGF control barrier function we monitored electrical resistance across a monolayer of primary human retinal endothelial cells (HRECs). Confluent, quiescent HRECs form a stable barrier (black tracing in Fig 1A). Adding a saturating dose of VEGF (1-2 nM) quickly (within minutes) relaxed the barrier (Fig 1A; red and green tracing). Following this acute barrier breakdown, barrier function was erratic for approximately 4 hr whereupon it stabilized for at least 60 hrs (Fig 1A and data not shown). Neutralizing VEGF with anti-VEGF (either aflibercept, or bevacizumab) completely restored barrier function (Fig 1A; green tracing and data not shown). We conclude that this experimental system is conducive to investigating the underlying mechanism by which VEGF relaxes the endothelial cell barrier and how anti-VEGF restores it. Furthermore, VEGF-mediated opening of the barrier proceeds through a process that takes hours to stabilize and is fully reversed by anti-VEGF.

We were surprised to observe that anti-VEGF further relaxed the barrier before closing it (Fig 1A). This phenomenon was observed routinely, although its magnitude was variable. Buffer alone, denatured anti-VEGF or an equivalent amount of an unrelated protein (bovine serum albumin) did not cause it to occur (data not shown). These results indicate that it is dependent on anti-VEGF, and suggests the barrier is not fully relaxed by prolonged exposure to a saturating dose of VEGF.

Varying the duration of exposure to VEGF, influenced how long it took anti-VEGF to re-close the barrier. In the experiment show in Fig 1A, it took 7 hrs for the barrier to reform after adding anti-VEGF to cells that had been exposed to VEGF for 8 hrs. Shortening or extending the duration of exposure to VEGF resulted in a corresponding change in how long it took to close the barrier after the addition of anti-VEGF (Fig 1B).

Journal Pre-proof

A simple explanation for the kinetics of anti-VEGF-mediated barrier closure is that it reflects the kinetics of VEGFR2 inactivation. However, we found that this was not the case. Addition of anti-VEGF to cells that had been exposed to VEGF for 24 hrs inactivated VEGFR2 much faster than it took to close the barrier (Fig 1B-D), and thereby suggested the anti-VEGF-mediated barrier closure required more than simply inactivating VEGFR2.

Together these observations support the concept that VEGF-mediated opening of the barrier is both progressive, and fully reversibly by anti-VEGF. Furthermore, while inactivating VEGFR2 is likely to initiate the process of barrier closure, these data suggest that anti-VEGF reverses additional VEGF-driven events.

VEGF/anti-VEGF regulated expression of genes that govern vascular homeostasis

Because prolonged exposure to VEGF alters expression of genes, including those that govern vascular homeostasis, we considered if changes in gene expression contributed to VEGF/anti-VEGF control of barrier function. To this end, we profiled the VEGF- and anti-VEGF-dependent changes in gene expression according to the experimental strategy shown in Fig 2A. The pie chart in Fig 2B illustrates the key findings of this RNAseq-based effort: VEGF altered expression of 4372 genes, and anti-VEGF overcame the effect of VEGF for 279 of these genes (complete and partial reversal for 162 and 117 genes, respectively). Fig 2C shows the magnitude of the VEGF- or anti-VEGF-driven change in expression for the top 32 genes.

The 279 anti-VEGF DEGs (differentially expressed genes) were subjected to MetaCore-based pathway analysis (Fig 2D). Anti-VEGF DEGs were most strongly and commonly found to belong to the cell cycle pathway, especially as it related to the G2/M phase. Furthermore, both the identity of the genes, and direction of the changes suggested that acute neutralization of

VEGF promotes transition of cells into G2/M. However, while VEGF modestly increased the percentage of the cells in S phase, anti-VEGF had no impact on G2/M (data not shown). This feeble effect of VEGF/anti-VEGF on the stage of cell cycle was expected for cells grown to confluence, which results in contact-dependent inhibition of cell cycle progression.

As a complementary approach to identify anti-VEGF DEGs that are necessary for anti-VEGF-mediated re-closure of the endothelial cell barrier we considered those anti-VEGF DEGs that are known to govern vascular homeostasis. To this end we assembled a list of genes that are included in twelve Qiagen RT^2 Profiler PCR Arrays: Human WNT Signaling Pathway, Human WNT Signaling Pathway Plus, Cell Junctions, Human TGFb / BMP Signaling Pathway Plus, Human TGFb / BMP Signaling Pathway, Human Notch Signaling Pathway Plus, Human Notch Signaling Pathway, Human Hippo Signaling Pathway, Human Endothelial Cell Biology, Human Cellular Senescence, Human Angiogenesis, and Human Adherens Junctions. The following genes were added to this list because recent publications demonstrate that they contribute to vascular homeostasis: PTPRB, FGD5, RHOB, PIK3CD, AKT1, AKT2, AKT3, PLCG1, MAPK3, MAPK1, SRC, FYN, YES1, UNC5B, ETV2 [26-34]. After eliminating the duplicates, 660 entries remained, which we designated as vascular homeostasis (VH) genes (Supplemental Table S1).

Fig 2E lists the 21 anti-VEGF DEGs that are also VH genes. We chose to pursue *ACE* (angiotensin converting enzyme) because the renin-angiotensin aldosterone system (RAAS) governs angiogenesis and/or endothelial cell barrier function in both experimental animals, and patients. RAAS antagonists protect diabetic animals from retinal vessel leakage [10-13]. Patients taking RAAS antagonists are less likely to develop diabetic retinopathy, and more prone to improve once they develop it [6, 7]. While animal studies demonstrated a correlation between

RAAS antagonism, prevention of diabetic retinopathy and lower levels of retinal VEGF, the underlying mechanism has not been elucidated. Furthermore, the role of RAAS in anti-VEGF-mediated barrier closure has not been addressed. As outlined below, we proceeded to develop and test the hypothesis that VEGF/anti-VEGF-mediated control of the endothelial cell barrier involves the RAAS (Fig 3A).

In summary, protracted exposure to VEGF increased expression of many genes, including those that are involved in barrier function, and anti-VEGF overcame a subset of these changes. These results identified candidate genes by which VEGF and anti-VEGF govern barrier function in the context of prolonged exposure to VEGF.

VEGF/anti-VEGF altered expression of members of the RAAS at times corresponding to changes in barrier function

To begin to test the hypothesis shown in Fig 3A we investigated whether VEGF and anti-VEGF altered expression of members of the RAAS pathway at times corresponding to changes in barrier function. This was not a given because the duration of VEGF/anti-VEGF exposure in the RNAseq experiments (Fig 2A) was not the same as the TEER experiments (Fig 1A). We observed that VEGF increased expression of *ACE* at times corresponding to barrier relaxation, and that anti-VEGF-driven restoration of barrier function was temporally aligned with a decline in *ACE* expression (Fig 1A and 3B). Furthermore, expression of some of the other genes that were both VH genes, and anti-VEGF DEGs did not temporally align with changes in barrier function (*EFNB2*, *STIL*, *CCNA2*; data not shown). In summary, *ACE*, a member of the RAAS is regulated by VEGF/anti-VEGF in a way and at times that support the working hypothesis shown in Fig 3A.

RAAS was one of the effectors by which VEGF relaxes the barrier

To test if the RAAS participated in VEGF-mediated barrier relaxation we antagonized members of the RAAS with inhibitors that are commonly used in patients. Trandolapril, an ACE inhibitor, reduced the responsiveness of cells to VEGF (Fig 4A,D). Similarly, valsartan, an antagonist of the angiotensin II (AII) receptor (AGTR1) that is expressed by endothelial cells, reduced VEGF-induced permeability (Fig 4 B,E). Additional ACE (ramipril) or AGTR1 (telmisartan) antagonists also impaired VEGF-induced barrier relaxation (Supplemental Figure S1). These agents had no effect on basal permeability (data not shown). Furthermore, a FITC-dextran-based approach to measure permeability confirmed that inhibiting the RAAS attenuated VEGF-induced permeability (Supplemental Figure S2). Finally, IL-1b-induced permeability was unaffected by ramipril or valsartan (Fig 4C,F).

This data set shows that antagonizing RAAS has a relatively small effect on VEGF's ability to relax the barrier. Increasing or decreasing the dose of the inhibitors did not increase the magnitude of their effect (Supplemental Figure S3A and B). Similarly, lowering the dose of VEGF, so that the barrier was only partially compromised, did not improve the efficacy of the drugs (Supplemental Figure S3C and D).

These data demonstrate that VEGF engages the RAAS to relax the barrier. Furthermore, because the effect of inhibiting the RAAS is partial, it appears that VEGF acts via additional effectors to relax the barrier in cells that are enduringly exposed to VEGF.

Activating the RAAS attenuated anti-VEGF-mediated closure of the barrier

Journal Pre-proof

While previous reports indicate a relationship between VEGF and RAAS, whether RAAS affects the efficacy of anti-VEGF has not been investigated. To this end, we tested if enforcing RAAS activity influenced anti-VEGF-mediated closure of the barrier by first relaxing the barrier with VEGF, and then adding anti-VEGF together with purified ACE or AII. Fig 5A,B shows that activating RAAS with purified ACE suppressed anti-VEGF's ability to re-close the barrier. Valsartan eliminated the effect of ACE indicating that activation of AGTR1 was required for this phenomenon. Addition of purified AII together with anti-VEGF also attenuated anti-VEGF's ability to close the barrier (Fig 5C,D). These data indicate that the status of the RAAS system influences anti-VEGF's efficacy; an activated RAAS suppresses anti-VEGF's ability to reclose the barrier.

We also tested if activating the RAAS was sufficient to relax the barrier. Addition of either purified ACE, or AII did not relax the barrier of cells under basal conditions (Supplemental Figure S4A and B). A plausible reason is that AGTR1 expression, which is increased by VEGF (data not shown), was not high enough under basal conditions to enable cells to respond to the added RAAS activators.

We performed the following experiments to determine if ACE or AII enhanced barrier relaxation in cells exposed to VEGF. Neither of the RAAS activators enhanced permeability driven by either a submaximal, or maximal concentration of VEGF (Supplemental Figure S4C and data not shown). Dose response experiments indicated that 0.5 nM VEGF opened the barrier to 50% of the level observed with a saturating concentration (1 nM) of VEGF (data not shown). Cells make *ACE* in response to VEGF (Fig 3), and hence it is possible that the amount of endogenously-produced ACE and AII sufficed to maximally activate the RAAS in VEGF-stimulated cells.

In conclusion, while exogenous RAAS activators did not influence basal or VEGF-driven permeability, they suppressed the ability of anti-VEGF to reclose the barrier that was opened by extended exposure to VEGF.

RAAS contributed to VEGF/anti-VEGF control of the barrier in an additional in vitro model.

For all of the experiments described thus far, we used high glucose (30 mM for at least 10 days)-treated HRECs, which is the most commonly used in vitro model of DM [35-38]. We repeated key experiments with a second in vitro model, namely one in which we exposed cells to fatty acids (50 uM palmitate) and cytokines (0.1 ng/ml TNFβ) for 24 hrs prior to the start of the experiments. Similar to high glucose, free fatty acids and cytokines are elevated in patients with DM [39-43]. Dose response experiments indicated that the chosen dose of palmitate and TNFβ did not alter either basal permeability, or VEGF/anti-VEGF-mediated barrier relaxation/closure (Supplemental Figure S5 and data not shown). Furthermore, antagonists of the RAAS reduced VEGF-induced permeability and RAAS activators suppressed the ability of anti-VEGF to reclose the barrier (Supplemental Figure S5). Taken together these results demonstrate that in multiple in vitro models of DM the RAAS is one of the effectors of VEGF, and that activating the RAAS blunts the efficacy of anti-VEGF.

Discussion

Using in vitro models of DM-induced endothelial dysfunction we made the following discoveries:

- The duration of exposure to VEGF influences both barrier relaxation, and anti-VEGF-mediated re-closure

- The vast majority of VEGF-induced changes in gene expression are not reversed by anti-VEGF
- VEGF uses multiple effectors to relax the endothelial cell barrier
- Activating the RAAS reduces the efficacy of anti-VEGF

The duration of exposure to VEGF influences both barrier relaxation and anti-VEGF-mediated closure. These observations suggest that VEGF-driven barrier relaxation is a process, which develops/matures as cells continue to be exposed to VEGF. For instance, activated VEGFR2 quickly engages signaling events that post-translationally modify existing components of adherens junctions [44-46]. These early events give way to changes in expression of genes that code for proteins that can further influence barrier function via a wide spectrum of mechanisms (Fig 5C). Regulators of the extracellular matrix, the cytoskeleton and components of the various types of junctions that connect endothelial cells all contribute to control of paracellular permeability [47-49]. Thus, the nature of the VEGF-breached endothelial barrier is in part dependent on how long cells have been exposed to VEGF. Consequently, anti-VEGF's mechanism of action will depend on the duration of exposure to VEGF. In diseases such as DR, which involve chronic elevation of VEGF, the anti-VEGF-mediated benefit (reduced permeability) is likely to involve not only inactivation of VEGFR2, but also change in gene expression.

By increasing production of ACE, VEGF triggers enduring permeability, which is a potential explanation for why anti-VEGF takes so long to re-close the EC barrier. While neutralizing VEGF occurs within minutes, it is likely to take longer for the elevated level of *ACE* mRNA and ACE protein, AII and AII-induced signaling to subside.

The vast majority (94%) of VEGF-induced changes in gene expression are not reversed by anti-VEGF. This observation provides an approach to identify those VEGF-regulated genes that govern barrier function, namely, those that are reversed by anti-VEGF. Furthermore, these genes are also candidate effectors of anti-VEGF. Finally, the realization that cells retain a molecular memory of VEGF (durable VEGF-induced changes in gene expression) suggest that this phenomenon may contribute to non-responsiveness to anti-VEGF. The endothelium within blood vessels that irreversibly express genes that VEGF engages to relax the barrier would be insensitive to anti-VEGF-based therapies to reverse leakage of blood vessels.

The finding that antagonizing the RAAS only partially inhibited VEGF-induced permeability indicates that VEGF engages multiple, non-redundant effectors to relax the barrier in cells that are exposed to VEGF for a prolonged time period. Identification of the RAAS as one of these effectors provides mechanistic insight into the previously reported relationship between the RAAS and VEGF [10-13].

Activating the RAAS reduces the efficacy of anti-VEGF. Thus, RAAS is like cytokines or the kallikrein system, which can open the barrier independently of VEGF and hence drive leakage in the face of anti-VEGF therapy[50, 51]. Unlike cytokines or the kallikrein system, patients with DR are often treated with inhibitors of the RAAS. The discovery that activated RAAS blunts the efficacy of anti-VEGF predicts that anti-VEGF will provide greater benefit to patients who are consuming RAAS antagonists. This is because such antagonists work together with anti-VEGF to re-close the barrier (Fig 5), and hence anti-VEGF constitutes the second arm of combo therapy. In contrast, anti-VEGF is simply monotherapy in patients who are not taking inhibitors of the RAAS. A clinical study comparing responsiveness to anti-VEGF in patients

who do and do not consume antagonists of the RAAS is an approach to address this intriguing possibility.

RAAS antagonists appear to differ in their benefit for patients with DR. A meta-analysis of patients with DR reported that ACE inhibitors reduced the risk of incidence and progression, and increased likelihood of regression, whereas AGTR1 blockers only increased the likelihood of regression [7]. In our in vitro model, we didn't observe an obvious difference in the two types of RAAS antagonists in preventing VEGF-induced leakage. While the strengths of this commonly-used in vitro model is its focus on endothelial cells [52, 53], its weakness is the absence of other VEGF-responsive cell types [35-38]. VEGFRs are expressed by multiple retinal cells types besides the endothelium, including ganglion cells, muller cells and amacrine cells [54]. The response of these non-endothelial cell types to neutralization of VEGF may contribute to the overall anti-VEGF effect that is observed in patients.

Acknowledgements

We thank members of the Kazlauskas lab (Anara Serikbaeva and Basma Baccouch) for their help editing the manuscript, and Lauren Kalinowski for generating the diagrams.

Journal Pre-proof

References

[1] Stitt AW, Curtis TM, Chen M, Medina RJ, McKay GJ, Jenkins A, Gardiner TA, Lyons TJ, Hammes HP, Simo R, Lois N: The progress in understanding and treatment of diabetic retinopathy. Prog Retin Eye Res 2016, 51:156-86.
[2] Hamilton SJ, Watts GF: Endothelial dysfunction in diabetes: pathogenesis, significance, and treatment. Rev Diabet Stud 2013, 10:133-56.
[3] Cheung N, Mitchell P, Wong TY: Diabetic retinopathy. Lancet 2010, 376:124-36.
[4] Yau JW, Rogers SL, Kawasaki R, Lamoureux EL, Kowalski JW, Bek T, Chen SJ, Dekker JM, Fletcher A, Grauslund J, Haffner S, Hamman RF, Ikram MK, Kayama T, Klein BE, Klein R, Krishnaiah S, Mayurasakorn K, O'Hare JP, Orchard TJ, Porta M, Rema M, Roy MS, Sharma T, Shaw J, Taylor H, Tielsch JM, Varma R, Wang JJ, Wang N, West S, Xu L, Yasuda M, Zhang X, Mitchell P, Wong TY, Meta-Analysis for Eye Disease Study G: Global prevalence and major risk factors of diabetic retinopathy. Diabetes care 2012, 35:556-64.
[5] Tight blood pressure control and risk of macrovascular and microvascular complications in type 2 diabetes: UKPDS 38. UK Prospective Diabetes Study Group. BMJ 1998, 317:703-13.
[6] Chaturvedi N, Sjolie AK, Stephenson JM, Abrahamian H, Keipes M, Castellarin A, Rogulja-Pepeonik Z, Fuller JH: Effect of lisinopril on progression of retinopathy in normotensive people with type 1 diabetes. The EUCLID Study Group. EURODIAB Controlled Trial of Lisinopril in Insulin-Dependent Diabetes Mellitus. Lancet 1998, 351:28-31.
[7] Wang B, Wang F, Zhang Y, Zhao SH, Zhao WJ, Yan SL, Wang YG: Effects of RAS inhibitors on diabetic retinopathy: a systematic review and meta-analysis. Lancet Diabetes Endocrinol 2015, 3:263-74.
[8] Bader M: Tissue renin-angiotensin-aldosterone systems: Targets for pharmacological therapy. Annu Rev Pharmacol Toxicol 2010, 50:439-65.
[9] George AJ, Thomas WG, Hannan RD: The renin-angiotensin system and cancer: old dog, new tricks. Nat Rev Cancer 2010, 10:745-59.
[10] Gilbert RE, Kelly DJ, Cox AJ, Wilkinson-Berka JL, Rumble JR, Osicka T, Panagiotopoulos S, Lee V, Hendrich EC, Jerums G, Cooper ME: Angiotensin converting enzyme inhibition reduces retinal overexpression of vascular endothelial growth factor and hyperpermeability in experimental diabetes. Diabetologia 2000, 43:1360-7.
[11] Kim JH, Kim JH, Yu YS, Cho CS, Kim KW: Blockade of angiotensin II attenuates VEGF-mediated blood-retinal barrier breakdown in diabetic retinopathy. J Cereb Blood Flow Metab 2009, 29:621-8.
[12] Ebrahimian TG, Tamarat R, Clergue M, Duriez M, Levy BI, Silvestre JS: Dual effect of angiotensin-converting enzyme inhibition on angiogenesis in type 1 diabetic mice. Arterioscler Thromb Vasc Biol 2005, 25:65-70.
[13] Phipps JA, Clermont AC, Sinha S, Chilcote TJ, Bursell SE, Feener EP: Plasma kallikrein mediates angiotensin II type 1 receptor-stimulated retinal vascular permeability. Hypertension 2009, 53:175-81.
[14] Nguyen QD, Brown DM, Marcus DM, Boyer DS, Patel S, Feiner L, Gibson A, Sy J, Rundle AC, Hopkins JJ, Rubio RG, Ehrlich JS, Rise, Group RR: Ranibizumab for diabetic macular edema: results from 2 phase III randomized trials: RISE and RIDE. Ophthalmology 2012, 119:789-801.

[15] Brown DM, Nguyen QD, Marcus DM, Boyer DS, Patel S, Feiner L, Schlottmann PG, Rundle AC, Zhang J, Rubio RG, Adamis AP, Ehrlich JS, Hopkins JJ, Ride, Group RR: Long-term outcomes of ranibizumab therapy for diabetic macular edema: the 36-month results from two phase III trials: RISE and RIDE. Ophthalmology 2013, 120:2013-22.
[16] Heier JS, Bressler NM, Avery RL, Bakri SJ, Boyer DS, Brown DM, Dugel PU, Freund KB, Glassman AR, Kim JE, Martin DF, Pollack JS, Regillo CD, Rosenfeld PJ, Schachat AP, Wells JA, 3rd, American Society of Retina Specialists Anti VfDMECEP: Comparison of Aflibercept, Bevacizumab, and Ranibizumab for Treatment of Diabetic Macular Edema: Extrapolation of Data to Clinical Practice. JAMA Ophthalmol 2016, 134:95-9.
[17] Diabetic Retinopathy Clinical Research N, Wells JA, Glassman AR, Ayala AR, Jampol LM, Aiello LP, Antoszyk AN, Arnold-Bush B, Baker CW, Bressler NM, Browning DJ, Elman MJ, Ferris FL, Friedman SM, Melia M, Pieramici DJ, Sun JK, Beck RW: Aflibercept, bevacizumab, or ranibizumab for diabetic macular edema. N Engl J Med 2015, 372:1193-203.
[18] Moreno-Munoz D, de la Haba-Rodriguez JR, Conde F, Lopez-Sanchez LM, Valverde A, Hernandez V, Martinez A, Villar C, Gomez-Espana A, Porras I, Rodriguez-Ariza A, Aranda E: Genetic variants in the renin-angiotensin system predict response to bevacizumab in cancer patients. Eur J Clin Invest 2015, 45:1325-32.
[19] Spector AA, Hoak JC: An improved method for the addition of long-chain free fatty acid to protein solutions. Anal Biochem 1969, 32:297-302.
[20] Li H: Aligning sequence reads, clone sequences and assembly contigs with BWA-MEM. arXiv 2013, arXiv 1303.3997v1 [q-bio.GN].
[21] Liao Y, Smyth GK, Shi W: featureCounts: an efficient general purpose program for assigning sequence reads to genomic features. Bioinformatics 2014, 30:923-30.
[22] McCarthy DJ, Chen Y, Smyth GK: Differential expression analysis of multifactor RNA-Seq experiments with respect to biological variation. Nucleic Acids Res 2012, 40:4288-97.
[23] Robinson MD, McCarthy DJ, Smyth GK: edgeR: a Bioconductor package for differential expression analysis of digital gene expression data. Bioinformatics 2010, 26:139-40.
[24] Benjamini Y, Hochberg, Y.: Controlling the False Discovery Rate: A Practical and Powerful Approach to Multiple Testing. J R Stat Soc Ser B Methodol 1995, 57:289–300.
[25] Senbabaoglu Y, Michailidis G, Li JZ: Critical limitations of consensus clustering in class discovery. Sci Rep 2014, 4:6207.
[26] Dominguez MG, Hughes VC, Pan L, Simmons M, Daly C, Anderson K, Noguera-Troise I, Murphy AJ, Valenzuela DM, Davis S, Thurston G, Yancopoulos GD, Gale NW: Vascular endothelial tyrosine phosphatase (VE-PTP)-null mice undergo vasculogenesis but die embryonically because of defects in angiogenesis. Proc Natl Acad Sci U S A 2007, 104:3243-8.
[27] Kurogane Y, Miyata M, Kubo Y, Nagamatsu Y, Kundu RK, Uemura A, Ishida T, Quertermous T, Hirata K, Rikitake Y: FGD5 mediates proangiogenic action of vascular endothelial growth factor in human vascular endothelial cells. Arterioscler Thromb Vasc Biol 2012, 32:988-96.
[28] Adini I, Rabinovitz I, Sun JF, Prendergast GC, Benjamin LE: RhoB controls Akt trafficking and stage-specific survival of endothelial cells during vascular development. Genes Dev 2003, 17:2721-32.
[29] Bijli KM, Fazal F, Slavin SA, Leonard A, Grose V, Alexander WB, Smrcka AV, Rahman A: Phospholipase C-epsilon signaling mediates endothelial cell inflammation and barrier disruption

in acute lung injury. American journal of physiology Lung cellular and molecular physiology 2016, 311:L517-24.
[30] Ricard N, Scott RP, Booth CJ, Velazquez H, Cilfone NA, Baylon JL, Gulcher JR, Quaggin SE, Chittenden TW, Simons M: Endothelial ERK1/2 signaling maintains integrity of the quiescent endothelium. J Exp Med 2019, 216:1874-90.
[31] Eliceiri BP, Paul R, Schwartzberg PL, Hood JD, Leng J, Cheresh DA: Selective requirement for Src kinases during VEGF-induced angiogenesis and vascular permeability. Mol Cell 1999, 4:915-24.
[32] Birukova AA, Shah AS, Tian Y, Gawlak G, Sarich N, Birukov KG: Selective Role of Vinculin in Contractile Mechanisms of Endothelial Permeability. Am J Respir Cell Mol Biol 2016, 55:476-86.
[33] Koch AW, Mathivet T, Larrivee B, Tong RK, Kowalski J, Pibouin-Fragner L, Bouvree K, Stawicki S, Nicholes K, Rathore N, Scales SJ, Luis E, del Toro R, Freitas C, Breant C, Michaud A, Corvol P, Thomas JL, Wu Y, Peale F, Watts RJ, Tessier-Lavigne M, Bagri A, Eichmann A: Robo4 maintains vessel integrity and inhibits angiogenesis by interacting with UNC5B. Dev Cell 2011, 20:33-46.
[34] Shah AV, Birdsey GM, Randi AM: Regulation of endothelial homeostasis, vascular development and angiogenesis by the transcription factor ERG. Vascular pharmacology 2016, 86:3-13.
[35] Roy S, Sala R, Cagliero E, Lorenzi M: Overexpression of fibronectin induced by diabetes or high glucose: phenomenon with a memory. Proc Natl Acad Sci U S A 1990, 87:404-8.
[36] Romeo G, Liu WH, Asnaghi V, Kern TS, Lorenzi M: Activation of nuclear factor-kappaB induced by diabetes and high glucose regulates a proapoptotic program in retinal pericytes. Diabetes 2002, 51:2241-8.
[37] El-Osta A, Brasacchio D, Yao D, Pocai A, Jones PL, Roeder RG, Cooper ME, Brownlee M: Transient high glucose causes persistent epigenetic changes and altered gene expression during subsequent normoglycemia. J Exp Med 2008, 205:2409-17.
[38] Chakravarthy U, Hayes RG, Stitt AW, McAuley E, Archer DB: Constitutive nitric oxide synthase expression in retinal vascular endothelial cells is suppressed by high glucose and advanced glycation end products. Diabetes 1998, 47:945-52.
[39] Lyons TJ, Jenkins AJ, Zheng D, Lackland DT, McGee D, Garvey WT, Klein RL: Diabetic retinopathy and serum lipoprotein subclasses in the DCCT/EDIC cohort. Invest Ophthalmol Vis Sci 2004, 45:910-8.
[40] Julius U: Influence of plasma free fatty acids on lipoprotein synthesis and diabetic dyslipidemia. Exp Clin Endocrinol Diabetes 2003, 111:246-50.
[41] Joussen AM, Poulaki V, Mitsiades N, Kirchhof B, Koizumi K, Dohmen S, Adamis AP: Nonsteroidal anti-inflammatory drugs prevent early diabetic retinopathy via TNF-alpha suppression. FASEB J 2002, 16:438-40.
[42] Abu el Asrar AM, Maimone D, Morse PH, Gregory S, Reder AT: Cytokines in the vitreous of patients with proliferative diabetic retinopathy. Am J Ophthalmol 1992, 114:731-6.
[43] Demircan N, Safran BG, Soylu M, Ozcan AA, Sizmaz S: Determination of vitreous interleukin-1 (IL-1) and tumour necrosis factor (TNF) levels in proliferative diabetic retinopathy. Eye (Lond) 2006, 20:1366-9.
[44] Dejana E: Endothelial adherens junctions: implications in the control of vascular permeability and angiogenesis. J Clin Invest 1997, 100:S7-10.

[45] Dejana E, Hirschi KK, Simons M: The molecular basis of endothelial cell plasticity. Nat Commun 2017, 8:14361.
[46] Claesson-Welsh L: Vascular permeability--the essentials. Ups J Med Sci 2015, 120:135-43.
[47] Schwartz MA, Vestweber D, Simons M: A unifying concept in vascular health and disease. Science 2018, 360:270-1.
[48] Augustin HG, Koh GY, Thurston G, Alitalo K: Control of vascular morphogenesis and homeostasis through the angiopoietin-Tie system. Nature reviews Molecular cell biology 2009, 10:165-77.
[49] Vestweber D: VE-cadherin: the major endothelial adhesion molecule controlling cellular junctions and blood vessel formation. Arterioscler Thromb Vasc Biol 2008, 28:223-32.
[50] Sohn HJ, Han DH, Kim IT, Oh IK, Kim KH, Lee DY, Nam DH: Changes in aqueous concentrations of various cytokines after intravitreal triamcinolone versus bevacizumab for diabetic macular edema. Am J Ophthalmol 2011, 152:686-94.
[51] Gao BB, Clermont A, Rook S, Fonda SJ, Srinivasan VJ, Wojtkowski M, Fujimoto JG, Avery RL, Arrigg PG, Bursell SE, Aiello LP, Feener EP: Extracellular carbonic anhydrase mediates hemorrhagic retinal and cerebral vascular permeability through prekallikrein activation. Nat Med 2007, 13:181-8.
[52] Kim D, Mouritzen U, Larsen BD, Roy S: Inhibition of Cx43 gap junction uncoupling prevents high glucose-induced apoptosis and reduces excess cell monolayer permeability in retinal vascular endothelial cells. Exp Eye Res 2018, 173:85-90.
[53] Stewart EA, Saker S, Amoaku WM: Dexamethasone reverses the effects of high glucose on human retinal endothelial cell permeability and proliferation in vitro. Exp Eye Res 2016, 151:75-81.
[54] Stitt AW, Simpson DA, Boocock C, Gardiner TA, Murphy GM, Archer DB: Expression of vascular endothelial growth factor (VEGF) and its receptors is regulated in eyes with intra-ocular tumours. The Journal of pathology 1998, 186:306-12.

Journal Pre-proof

Figure Legends

Figure 1. Signaling events did not appear to fully account for how VEGF/anti-VEGF governed the barrier in response to prolonged exposure to VEGF.

(A) The trans-endothelial electrical resistance (TEER) of confluent monolayers of HRECs was measured for 8 hrs following the addition of either VEGF vehicle, or VEGF (1 nM). At the 8 hr time point cells received either anti-VEGF (500 nM aflibercept), or aflibercept buffer, and then TEER was monitored for an additional 14 hrs. A high TEER value indicates effective barrier function, i.e. low permeability. The data are expressed as the mean ± SD (n=3-4).

(B) The type of experiment shown in panel A was repeated varying the duration of exposure to VEGF prior to addition of anti-VEGF. Plotting the resulting data revealed a linear relationship between the duration of exposure to VEGF and how long it took the barrier to close after adding anti-VEGF; Pearson correlation test: r = 0.92, p = 8.63*10^-08.

(C/D) Confluent monolayers of cells were exposed to VEGF (1 nM) for 24 h, whereupon anti-VEGF (500 nM aflibercept) was added for the indicated length of time. The cells were lysed and total cell lysates were subjected to Western blot analysis using the indicated antibodies. A representative experiment is shown in panel C. The extent of VEGFR2 phosphorylation was quantified and normalized to the level of total VEGFR2. Data from 3 independent experiments (mean ± SD) are shown in panel D.

Figure 2. VEGF changed the expression of vascular homeostasis genes, and such changes were overcome by anti-VEGF.

(A) Outline of the experimental strategy. Triplicate dishes of confluent HRECs were exposed to VEGF vehicle, VEGF (1 nM) or VEGF followed by anti-VEGF (500 nM aflibercept) for the

indicated duration, whereupon cells were harvested, RNA was isolated and subjected to RNAseq analysis. Differentially expressed genes (DEGs) were identified by pair-wise comparison between experimental groups as indicated in the diagram.

(B) The resulting RNAseq data are presented as a pie chart. VEGF induced a statistically significant ($p<0.05$) change in expression of 4372 genes; these are VEGF DEGs. Anti-VEGF overcame the VEGF-driven change for 279 of these genes; these are the anti-VEGF DEGs.

(C) A heatmap of the top 32 anti-VEGF DEGs, which are arranged according to the level of fold change (FC). The expression level is indicated by color; blue is low and red is high.

(D) The 279 anti-VEGF DEGs were subjected to MetaCore-based pathway analysis. The top 20 pathways, sorted according to statistical significance, are presented. The colors designate a type of pathway, for instance, green is for "cell cycle".

(E) The 21 of the 279 anti-VEGF DEGs that are known to govern vascular homeostasis are listed.

Figure 3. Temporal alignment of VEGF/anti-VEGF-induced changes in gene expression and barrier function.

A) Diagram of the working hypothesis. VEGF increases expression of angiotensin converting enzyme (ACE) and thereby converts angiotensin I (AI) into angiotensin II (AII), which binds to its receptor (encoded by the AGTR1 gene) and relaxes the barrier. By neutralizing VEGF, anti-VEGF reduces expression of ACE and thereby restores barrier function.

(B) Triplicate dishes of cells treated as described in the legend of Fig 1A were harvested, RNA was extracted and subjected to qRT-PCR using primers specific for *ACE*. Data are mean ± SD, n=3. The level of expression in unstimulated cells (black bars) was set to 1.0. For VEGF-treated

cells (red bars) the data are expressed as fold increase over unstimulated cells; **p<0.01, ***p<0.001, ****p<0.0001. The green bars indicate the expression in cells that were first treated with VEGF and then anti-VEGF; ††††p<0.0001, VEGF 8 h-treated group versus anti-VEGF group. Similar results we observed in three independent experiments.

Figure 4. Antagonizing RAAS attenuated VEGF-induced relaxation of the endothelial barrier. TEER measurements of VEGF-stimulated HRECs pre-treated with **(A/D)** trandolapril (ACE inhibitor) or **(B/E)** valsartan (AGTR1 inhibitor). Following a 2 h pre-treatment with trandolapril (100 nM), valsartan (1uM) or drug vehicle (DMSO), 2 nM of VEGF was added (indicated by the black arrow) and TEER recorded for 20 h. Data are expressed as a fraction of basal TEER, which was measured at the 0 time point. In panels D and E the area under the curve for the entire time course was quantified, normalized to the VEGF vehicle-treated cells and presented as the mean ± SD for a single representative experiment. **(C/F)** Same as panels A/B/D/E, except that the cells were exposed to IL-1β (20 ng/ml) instead of VEGF. Similar results were observed in at least three independent experiments. *p<0.05, **p<0.01.

Figure 5. Activating RAAS diminished anti-VEGF-mediated closure of the barrier.
(A/C) The TEER was measured as described in the legend of Figure 1A for cells exposed to VEGF (2 nM) for about 7 hrs followed by either anti-VEGF vehicle (red line), anti-VEGF (1 uM, green line), **(A)** anti-VEGF together with purified ACE (2 ug/ml, blue line), anti-VEGF together with ACE (2 ug/ml) and valsartan (1 uM, purple line), **(C)** or anti-VEGF together with angiotensin II (AII, 100 uM). Data are expressed as fraction of the starting (basal) TEER value (0 time point).

(B/D) The area under the curve in Fig 5A,C was quantified and normalized to the group that received VEGF alone (red lines in Fig 5A,C). Error bars indicate ± SD (*p<0.05, **p<0.01, ****p<0.0001, between indicated groups, n=3).

(E) VEGF activates its receptor and quickly engages signaling events that act on preexisting components of intracellular junctions to relax the barrier. Continued exposure to VEGF leads to changes in expression of genes that code for proteins that are also capable of regulating barrier function.

Journal Pre-proof

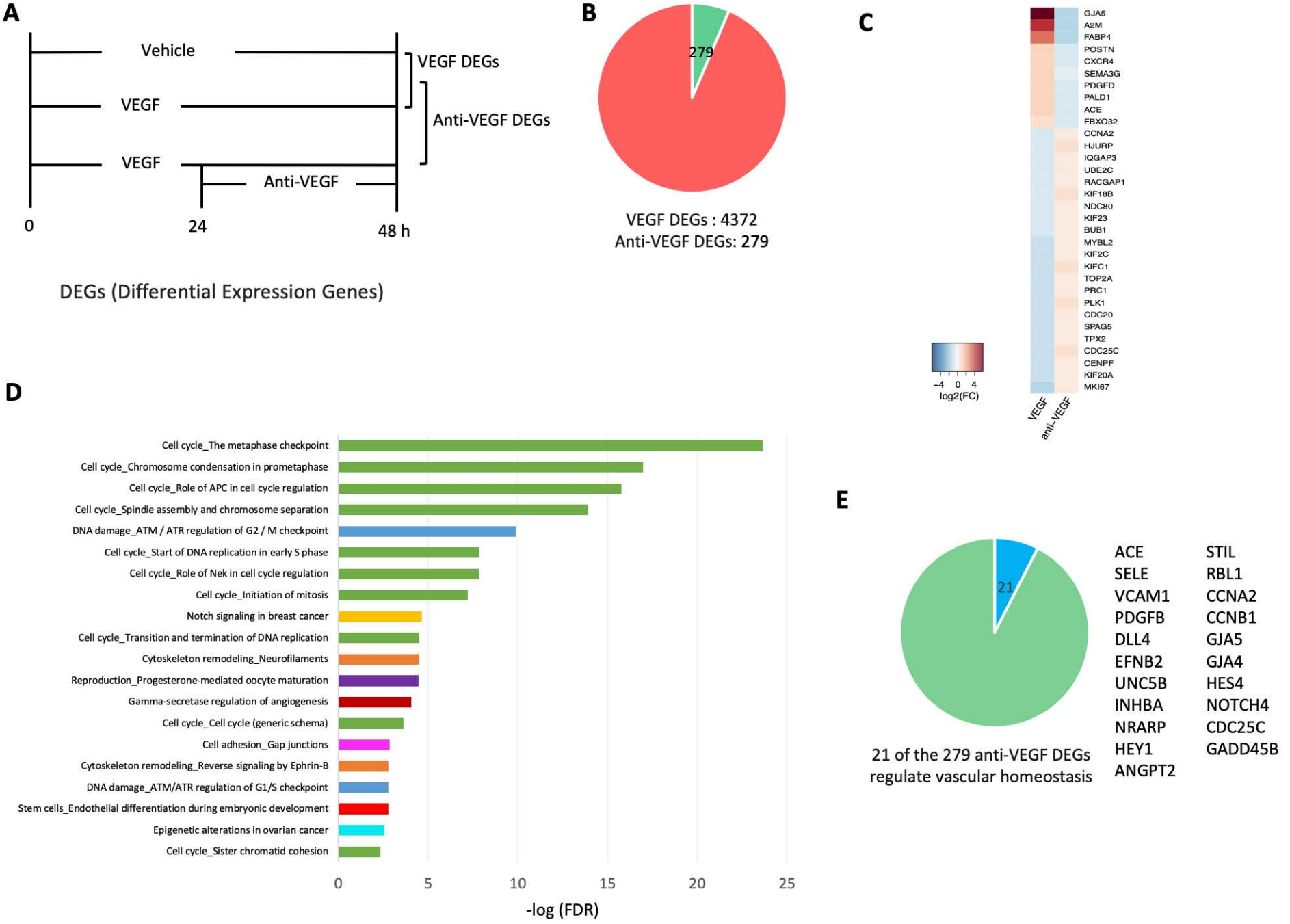
A
Vehicle
VEGF
VEGF
Anti-VEGF
VEGF DEGs
Anti-VEGF DEGs
0
24
48 h
DEGs (Differential Expression Genes)
B
279
VEGF DEGs : 4372
Anti-VEGF DEGs: 279
C
GJA5
A2M
FABP4
POSTN
CXCR4
SEMA3G
PDGFD
PALD1
ACE
FBXO32
CCNA2
HJURP
IQGAP3
UBE2C
RACGAP1
KIF18B
NDC80
KIF23
BUB1
MYBL2
KIF2C
KIFC1
TOP2A
PRC1
PLK1
CDC20
SPAG5
TPX2
CDC25C
CENPF
KIF20A
MKI67
−4 0 4
log2(FC)
VEGF
anti-VEGF
D
Cell cycle_The metaphase checkpoint
Cell cycle_Chromosome condensation in prometaphase
Cell cycle_Role of APC in cell cycle regulation
Cell cycle_Spindle assembly and chromosome separation
DNA damage_ATM / ATR regulation of G2 / M checkpoint
Cell cycle_Start of DNA replication in early S phase
Cell cycle_Role of Nek in cell cycle regulation
Cell cycle_Initiation of mitosis
Notch signaling in breast cancer
Cell cycle_Transition and termination of DNA replication
Cytoskeleton remodeling_Neurofilaments
Reproduction_Progesterone-mediated oocyte maturation
Gamma-secretase regulation of angiogenesis
Cell cycle_Cell cycle (generic schema)
Cell adhesion_Gap junctions
Cytoskeleton remodeling_Reverse signaling by Ephrin-B
DNA damage_ATM/ATR regulation of G1/S checkpoint
Stem cells_Endothelial differentiation during embryonic development
Epigenetic alterations in ovarian cancer
Cell cycle_Sister chromatid cohesion
0
5
10
15
20
25
-log (FDR)
E
21
21 of the 279 anti-VEGF DEGs
regulate vascular homeostasis
ACE
SELE
VCAM1
PDGFB
DLL4
EFNB2
UNC5B
INHBA
NRARP
HEY1
ANGPT2
STIL
RBL1
CCNA2
CCNB1
GJA5
GJA4
HES4
NOTCH4
CDC25C
GADD45B

A

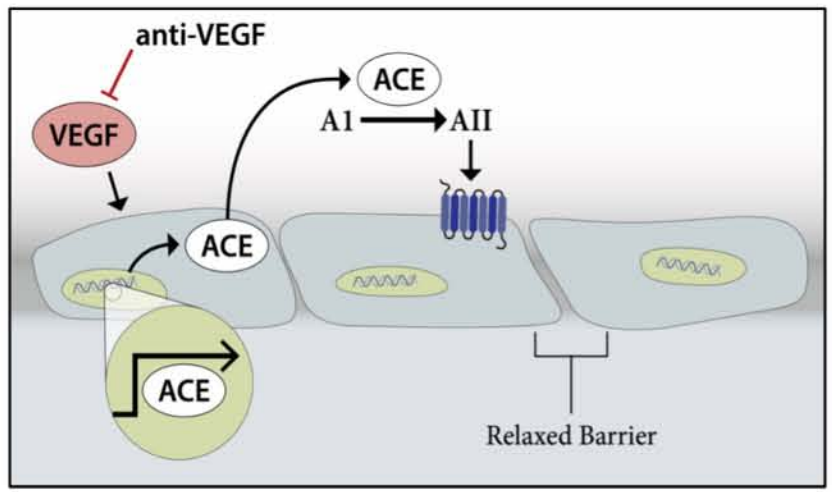
anti-VEGF
VEGF
ACE
A1
AII
ACE
ACE
Relaxed Barrier

B

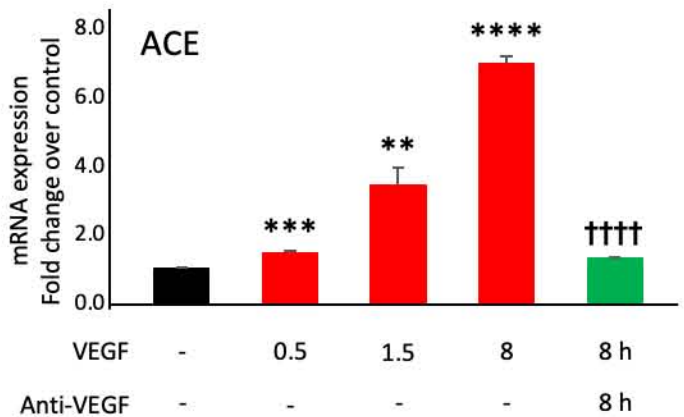
ACE
mRNA expression
Fold change over control
8.0
6.0
4.0
2.0
0.0
***
**
****
††††
VEGF - 0.5 1.5 8 8 h
Anti-VEGF - - - - 8 h

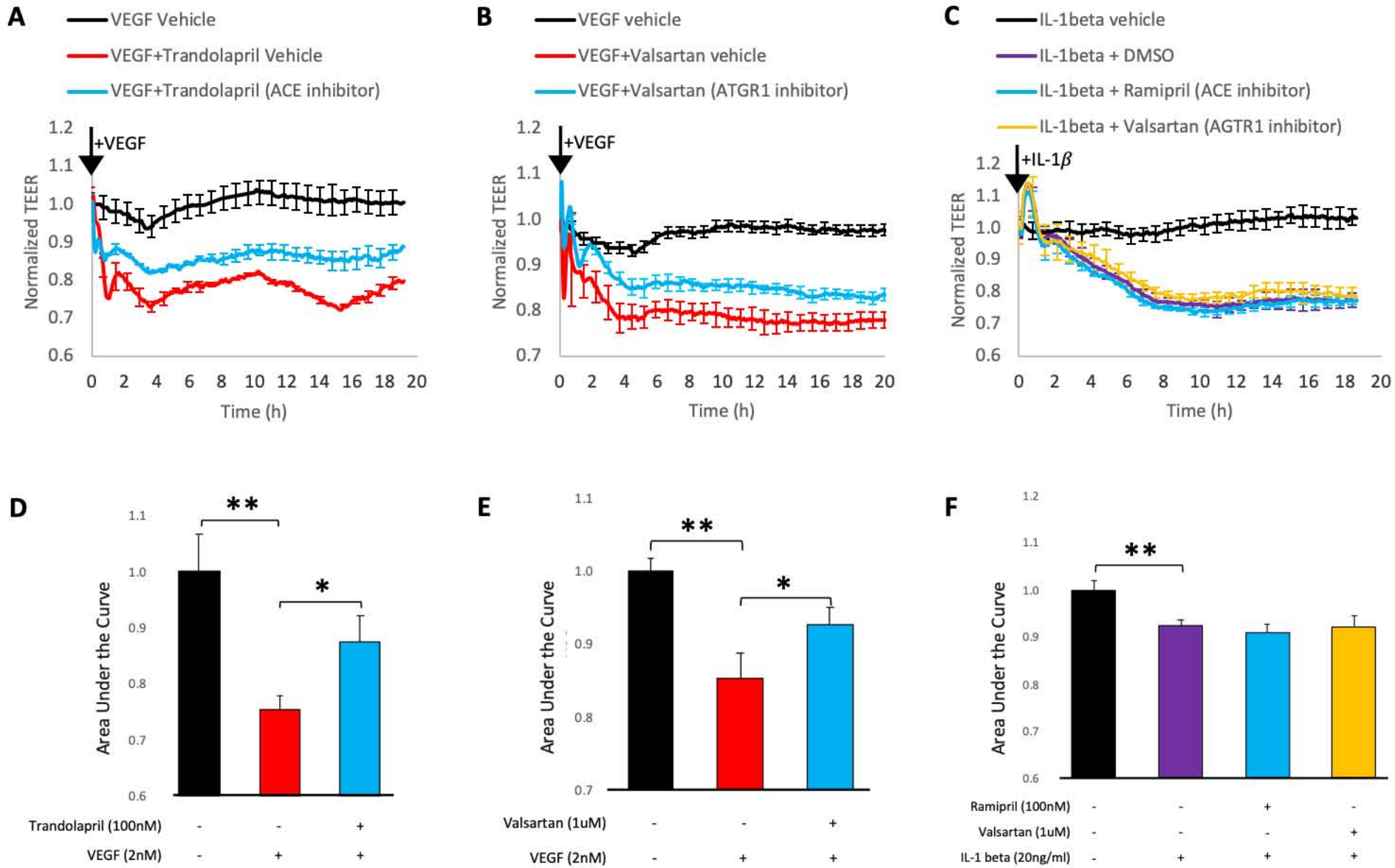
A
VEGF Vehicle
VEGF+Trandolapril Vehicle
VEGF+Trandolapril (ACE inhibitor)
+VEGF
Normalized TEER
Time (h)
B
VEGF vehicle
VEGF+Valsartan vehicle
VEGF+Valsartan (ATGR1 inhibitor)
+VEGF
Normalized TEER
Time (h)
C
IL-1beta vehicle
IL-1beta + DMSO
IL-1beta + Ramipril (ACE inhibitor)
IL-1beta + Valsartan (AGTR1 inhibitor)
+IL-1β
Normalized TEER
Time (h)
D
Area Under the Curve
Trandolapril (100nM)
VEGF (2nM)
E
Area Under the Curve
Valsartan (1uM)
VEGF (2nM)
F
Area Under the Curve
Ramipril (100nM)
Valsartan (1uM)
IL-1 beta (20ng/ml)

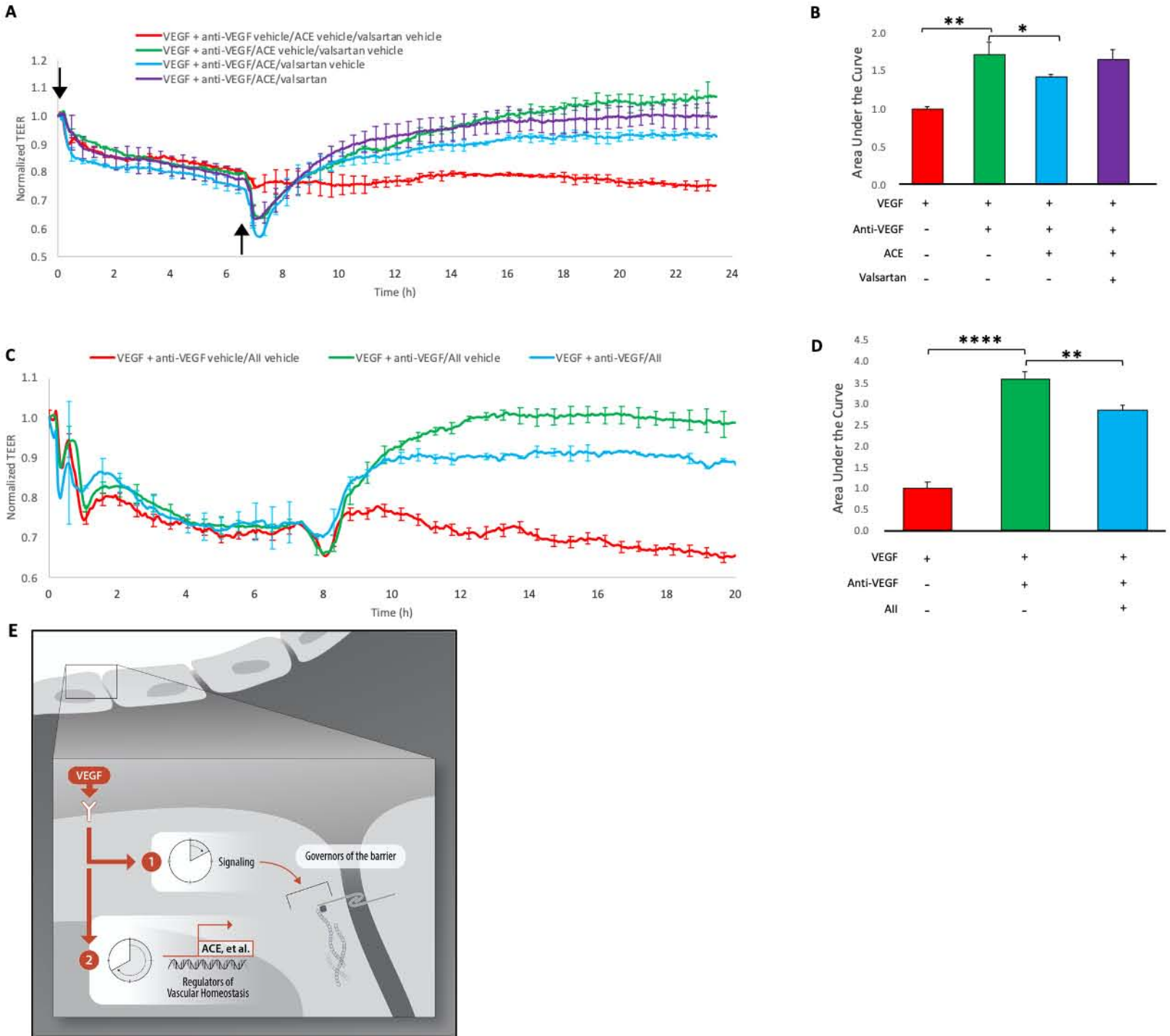
A
VEGF + anti-VEGF vehicle/ACE vehicle/valsartan vehicle
VEGF + anti-VEGF/ACE vehicle/valsartan vehicle
VEGF + anti-VEGF/ACE/valsartan vehicle
VEGF + anti-VEGF/ACE/valsartan
Normalized TEER
Time (h)
B
Area Under the Curve
**
*
VEGF
Anti-VEGF
ACE
Valsartan
C
VEGF + anti-VEGF vehicle/AII vehicle
VEGF + anti-VEGF/AII vehicle
VEGF + anti-VEGF/AII
Normalized TEER
Time (h)
D
Area Under the Curve
****
**
VEGF
Anti-VEGF
AII
E
VEGF
Signaling
Governors of the barrier
ACE, et al.
Regulators of
Vascular Homeostasis